

Optimizing Wireless Charger Placement for Directional Charging

Haipeng Dai Xiaoyu Wang Alex X. Liu Huizhen Ma Guihai Chen

State Key Laboratory for Novel Software Technology, Nanjing University, Nanjing, Jiangsu 210024, CHINA

{haipengdai, alexliu, gchen}@nju.edu.cn, {mg1633074, mg1533037}@smail.nju.edu.cn

Abstract—Wireless Power Transfer (WPT) technology has witnessed huge development because of its convenience and reliability. This paper concerns the fundamental issue of wireless charger PLacement with Optimized charging uTility (PLOT), that is, given a fixed number of chargers and a set of points on the plane, determining the positions and orientations of chargers such that the overall expected charging utility for all points is maximized. To address PLOT, we propose a $1 - 1/e - \epsilon$ approximation algorithm. First, we present techniques to approximate the nonlinear charging power and the expected charging utility to make the problem almost linear. Second, we develop a Dominating Coverage Set extraction method to reduce the continuous search space of PLOT to a limited and discrete one without performance loss. Third, we prove that the reformulated problem is essentially maximizing a monotone submodular function subject to a matroid constraint, and propose a greedy algorithm to address this problem. We conduct both simulation and field experiments to validate our theoretical results, and the results show that our algorithm can outperform comparison algorithms by at least 46.3%.

I. INTRODUCTION

Wireless Power Transfer (WPT) technology has witnessed huge development and advancement in recent times because of its advantages of no wiring, no contact, reliable and continuous power supply, and ease of maintenance. Wireless Power Consortium, an organization that aims to promote standardization of WPT, has grown to contain 213 member companies in 2016 including Microsoft, Qualcomm, Samsung, and Huawei [1]; and according to a recent report, wireless power transmission market is estimated to grow 17.04 billion to 2020 [2]. To achieve efficient energy transfer, WPT generally requires highly directional transmission by using high-gain and directional antennas for power transmitters and receivers to focus the energy in narrow energy beams, such as in millimeter wave cellular networks [3], [4], wireless rechargeable sensor networks [5], simultaneous wireless information and power transfer networks [6], [7], and wireless powered communication network [8]. Consequently, a power receiver, or called *rechargeable device*, can only receive non-negligible power from a power transmitter, or called *wireless charger*, when they are located in the covered regions of directional antennas of each other. Taking Figure 1 as an example, the device o_j can receive non-zero power from the wireless charger s_i while the device o_k cannot.

In this paper, we are concerned with the problem of wireless charger PLacement with Optimized charging uTility (PLOT). In our considered scenario, devices can appear at some known points on the plane with any orientation. Given a determined

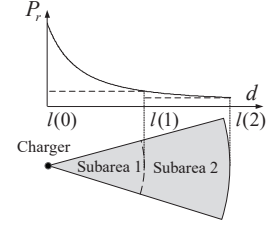
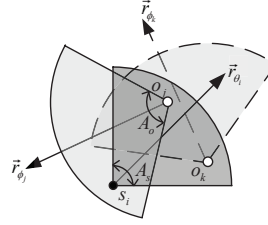


Fig. 1: Directional charging Fig. 2: Power approximation model

wireless charger topology, with different orientations, devices at a given point would receive different charging power, which leads to different degree of usefulness called *charging utility* in this paper. Then, the expected charging utility for devices at a point is the expected value of charging utility for devices whose orientations are uniformly distributed in $[0, 2\pi)$. Formally, given a fixed number of chargers and a set of points on the plane, the PLOT problem is to deploy the chargers on the plane, *i.e.*, to determine their positions and orientations (the combination of which we define as *strategies*), such that the overall expected charging utility for all points is maximized.

Though there have emerged some wireless charger placement schemes, none of them adopts the directional charging model for devices and is suitable for our problem. In addition, though there are some schemes considering the directional sensor placement problem, which is also close to ours, none of them can be adapted to address our problem. This is because essentially the directional sensor placement problem is a linear and geometric problem, and all its schemes assume an omnidirectional model for devices, which contradicts ours.

The PLOT problem has two main technical challenges. The first challenge is that the problem is essentially nonlinear and continuous. The problem is nonlinear because the charging power is nonlinear with distance, the utility function is nonlinear with power, and the expected charging utility for a point is an integral of charging utility from 0 to 2π . It is also continuous because both the positions and orientations of chargers are continuous values. The second challenge is to develop an approximation algorithm, which needs to bound the performance gap to the optimal one.

We propose an algorithm to address the above two challenges. First, we approximate the nonlinear charging power as piecewise constant, and approximate the expected charging utility for a point as the sum of utility from a limited number of devices. The objective function of the problem thus becomes

almost linear. Then, we develop a Dominating Coverage Set extraction method to reduce the continuous search space of strategies of chargers to a limited number of strategies without performance loss. Therefore, our problem becomes selecting a fixed number of strategies from a set of candidate ones to maximize the overall charging utility, which is discrete. We thus address the first challenge. Second, we prove that the reformulated problem falls into the scope of the problem of maximizing a monotone submodular function subject to matroid constraints, which allows a greedy algorithm to achieve a constant approximation ratio. Next, we bound the performance loss during the problem reformulation, and finally obtain the approximation ratio of our proposed algorithm. Thereby, we address the second challenge.

We conducted simulations and field experiments to evaluate our proposed algorithm. The simulation and field experimental results show that our algorithm can outperform comparison algorithms by at least 46.3% and at least 56.6%, respectively.

II. RELATED WORK

Wireless charger placement problem. All existing works considering the wireless charger placement problem adopt the omnidirectional charging model for devices and even chargers, rendering them not applicable to our problem. He *et al.* [9] considered charger placement for which static or mobile tags can receive sufficient power to keep continuous working. Chiu *et al.* [10] exploited the mobility nature of sensor nodes to improve charger deployment. Dai *et al.* [11] concerned the electromagnetic radiation safety issues for wireless charger placement.

Directional sensor placement problem. Directional sensor placement problem is one of the closest problems to ours. However, it is essentially a linear and geometric problem, and all related works on this problem assumed that devices are omnidirectional, which contradicts our model in this paper. In [12]–[14], the network plane is considered to be a grid, and any square of the grid is a candidate place for a directional sensor. Fusco *et al.* [15] focused on adjusting the orientation of sensors located at pre-determined positions to maximize the number of covered targets. Osais *et al.* [16] studied the problem of jointly deploying directional sensors and base stations to some of the candidate points to minimize the network-wide overhead. Han *et al.* [17] considered deploying a minimum number of directional sensors to cover targets while the sensors are allowed to deploy at any point in the area.

III. PROBLEM FORMULATION

A. Network Model and Charging Model

Suppose we have N points denoted as $O = \{o_1, o_2, \dots, o_N\}$ in a 2D plane Ω on which rechargeable devices may be placed with any orientation. We also have M directional wireless chargers, denoted as $S = \{s_1, s_2, \dots, s_M\}$, which can be placed anywhere with any orientation in the plane. By abuse of notation, we still use o_j to denote a rechargeable device, and

TABLE I: Notations

Symbol	Meaning
s_i	Wireless charger i , or its position
o_j	Point j to be charged, or wireless rechargeable device j
M	Number of wireless chargers to be deployed
N	Number of points to charge
A_s	Charging angle of chargers
A_o	Receiving angle of devices
θ_i	Orientation of charger s_i
ϕ_j	Orientation of device o_j
$P_r(\cdot)$	Charging power function
P_{th}	Threshold for charging utility function
α, β	Constants in the charging model
D	Farthest distance a charger can reach
$\mathcal{U}(\cdot)$	Utility function

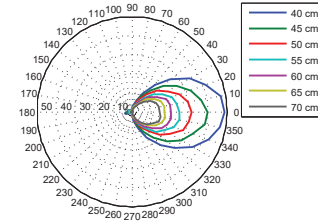


Fig. 3: Charging power vs. distance

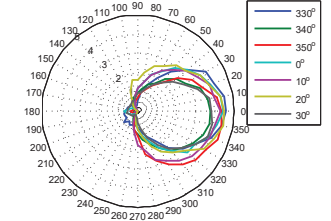


Fig. 4: Charging power vs. orientation angle

s_i to denote the position of charger s_i . We list the notations used in this paper in Table I.

We build our charging model by empirical studies. We use a commodity off-the-shelf TX91501 wireless charger and a rechargeable sensor node equipped with a P2110 power receiver both produced by Powercast [18], [19]. First, we let the sensor node always face to the charger, and vary the distance of the node from 40 cm to 70 cm and the charger's orientation angle with respect to the line connecting the charger and the node from 0° to 360° . We plot the experimental results in Figure 3 which shows that the node receives notable power only when it is within the span of a 60° sector, and negligibly small one elsewhere. Second, we fix the distance to 1 m, and vary the charger's orientation angle and the node's orientation angle (with respect to the line connecting the charger and the node) from -30° (330°) to 30° and from 0° to 350° , respectively. Figure 4 shows that the node receives notable charging power only when its orientation angle is within the range from -60° to 60° .

After all, we propose the directional charging model as follows. As demonstrated in Figure 1, a charger s_i with orientation vector \vec{r}_{θ_i} only charges devices with non-zero power in a (power) charging area in the shape of a sector with (power) charging angle A_s and radius D . A rechargeable device o_j with orientation vector \vec{r}_{ϕ_j} only receives non-zero power in a (power) receiving area in the shape of a sector with (power) receiving angle A_o and the same radius D . By incorporating the widely accepted empirical charging model proposed in [20], [21], and also following our experimental results, the charging power from the charger s_i to the device o_j can be given by

$$P_r(s_i, \theta_i, o_j, \phi_j) = \begin{cases} \frac{\alpha}{(\|s_i o_j\| + \beta)^2}, & 0 \leq \|s_i o_j\| \leq D, \\ \frac{s_i o_j \cdot \vec{r}_{\theta_i} - \|s_i o_j\| \cos(A_s/2) \geq 0,}{\text{and } \frac{o_j s_i \cdot \vec{r}_{\phi_j} - \|o_j s_i\| \cos(A_o/2) \geq 0.} & \\ 0, & \text{otherwise} \end{cases}$$

where α and β are two constants determined by the surrounding environment and the hardware parameters of chargers [20]–[22], $\|s_i o_j\|$ denotes the distance between s_i and o_j , A_s is the charging angle of chargers, A_o is the receiving angle of devices, and \vec{r}_{θ_i} and \vec{r}_{ϕ_j} are the unit vectors denoting the orientations of the charger and the device, respectively.

When a device o_j is charged by multiple wireless chargers, we assume the received power of o_j is the sum of the received power from all chargers [9].

B. Charging Utility Model

In practice, rechargeable devices typically have an upper bound for their truly received or required power due to hardware constraints or practical demand. Therefore, we present the following *charging utility* model to capture such characteristics.

$$\mathcal{U}(x) = \begin{cases} c_u \cdot x, & x \leq P_{th} \\ c_u \cdot P_{th}, & x > P_{th} \end{cases} \quad (1)$$

where c_u and P_{th} are predetermined constants, and usually we set $c_u = 1/P_{th}$ for normalization. In this model, the charging utility is first proportional to the charging power, and then becomes constant when the charging power exceeds the threshold P_{th} .

Based on the above charging utility model, the (*expected*) *charging utility* for a given point o_j is the expected value of charging utility for rechargeable devices at this point with their orientations uniformly distributed in the range of $[0, 2\pi)$, namely

$$\int_0^{2\pi} \frac{1}{2\pi} \mathcal{U}(\sum_{i=1}^M P_r(s_i, \theta_i, o_j, \phi)) d\phi. \quad (2)$$

Note that here s_i and θ_i ($i = 1, 2, \dots, M$) denote the positions and orientations of placed wireless chargers, respectively.

C. Problem Formulation

Let the tuple $\langle s_i, \theta_i \rangle$ denote the position s_i and orientation θ_i of the charger s_i , called *strategy* of the charger. We define the overall charging utility as the normalized sum of charging utility from all N points, i.e., $\frac{1}{N} \sum_{j=1}^N \int_0^{2\pi} \frac{1}{2\pi} \mathcal{U}(\sum_{i=1}^M P_r(s_i, \theta_i, o_j, \phi)) d\phi = \frac{1}{2\pi N} \sum_{j=1}^N \int_0^{2\pi} \mathcal{U}(\sum_{i=1}^M P_r(s_i, \theta_i, o_j, \phi)) d\phi$. Finally, our task is to determine the strategies for all the M chargers so that the overall charging utility is optimized. With all above, we define the wireless charger Placement with Optimized charging utility (PLOT) as follows.

$$\begin{aligned} \text{(P1)} \quad \max \quad & \frac{1}{2\pi N} \sum_{j=1}^N \int_0^{2\pi} \mathcal{U}(\sum_{i=1}^M P_r(s_i, \theta_i, o_j, \phi)) d\phi \\ \text{s.t.} \quad & s_i \in \Omega, 0 \leq \theta_i < 2\pi. \end{aligned}$$

Since the objective function of **P1** is nonlinear and the constraints are continuous, PLOT falls in the realm of nonlinear programs which are NP-hard [23]. Therefore, we have

Theorem 3.1: The PLOT problem **P1** is NP-hard.

IV. SOLUTION

In this subsection, we present our algorithm with approximation ratio $1 - 1/e - \epsilon$ to address PLOT. Generally, the PLOT algorithm consists of three steps. First, we use a piecewise constant function to approximate nonlinear charging power, and approximate the charging utility for a point as the sum of charging utility from a limited number of devices. By this means, the charging area of a charger is partitioned into many subareas. Second, we present a Dominating Coverage Set extraction method to reduce the continuous search space of strategies of chargers to a limited number of strategies without performance loss. The problem is then transferred into finding M strategies among the obtained strategies to maximize the overall charging utility. Third, we prove the reformulated problem falls in the realm of maximizing a monotone sub-modular optimization problem subject to a uniform matroid, and propose a greedy algorithm with performance guarantee to address this problem.

A. Area Discretization

1) Piecewise Constant Approximation of Charging Power:

Let $P_r(d)$ denote the power that a device receives from a charger with distance d , and suppose that their orientations are sufficiently close to each other such that $P_r(d) = \frac{\alpha}{(d+\beta)^2}$ when $0 \leq d \leq D$ and $P_r(d) = 0$ otherwise. We use multiple piecewise constant segments $\tilde{P}_r(d)$ to approximate the charging power $P_r(d)$. Our goal is to bound the approximation error and the computational overhead.

Figure 2 illustrates the key idea of the approximation of $P_r(d)$. Let $l(0), l(1), \dots, l(K)$ be the end points of K constant segments in an increasing sequence. Here, K is the number of segments that controls the approximation error. Obviously, with a larger K , the approximation error will be reduced, but more computational overhead will be introduced. In Figure 2, K is set to 2, and the black dotted curves stand for the approximated value of charging power.

Definition 4.1: Setting $l(0) = 0$ and $l(K) = D$, the piecewise constant function $\tilde{P}_r(d)$ can be defined as

$$\tilde{P}_r(d) = \begin{cases} P_r(l(1)), & d = l(0) \\ P_r(l(k)), & l(k-1) < d \leq l(k) \quad (k = 1, \dots, K) \\ 0, & d > l(K) \end{cases}$$

The following theorem offers the sufficient condition to ensure that the approximation error is less than ϵ_1 . We omit most proofs of lemmas and theorems in this paper to save space.

Theorem 4.1: Setting $l(0) = 0$, $l(K) = D$, and $l(k) = \beta((1 + \epsilon_1)^{k/2} - 1)$, ($k = 1, \dots, K - 1$) (therefore $K = \lceil \frac{\ln(P_r(0)/P_r(D))}{\ln(1 + \epsilon_1)} \rceil$), we have the approximation error as

$$1 \leq \frac{P_r(d)}{\tilde{P}_r(d)} \leq 1 + \epsilon_1, \quad (d \leq D). \quad (3)$$

2) Charging Utility Approximation for a Point: We present another technique to approximate the charging utility for a point to ease the problem. As Figure 5 shows, we use $\frac{2\pi}{\Delta A_o}$ rechargeable devices centered at a given point o_1 with orientations uniformly distributed in $[0, 2\pi)$ with even space ΔA_o to approximate all possible orientations of devices located at the point o_1 .

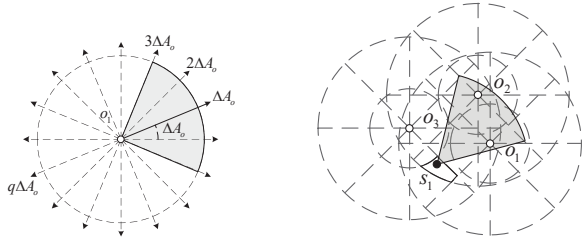


Fig. 5: Charging utility approx- Fig. 6: Plane discretization imation

After such approximation, the calculation of charging utility for a given point as expressed in Eq. (2) is simplified from an integral to a weighted sum, *i.e.*,

$$\frac{\Delta A_o}{2\pi A_o} \sum_{q=1}^{\frac{2\pi}{\Delta A_o}} \mathcal{U} \left(\sum_{i=1}^M P_r(s_i, \theta_i, o_j, q\Delta A_o) \right). \quad (4)$$

We note that though such approximation incurs performance loss, we show in the proof to Theorem 4.5 that such loss can be bounded.

3) *Discretizing the 2D Area*: In this subsection, we show how to discretize the 2D area based on the piecewise constant approximation of $P_r(d)$ and the charging utility approximation for a point, and therefore, confine the solution space.

The basic idea of area discretization is shown in Figure 6. We draw concentric circles with radius $l(1), l(2), \dots, l(K)$ centered at each device, respectively. Due to geometric symmetry, if a charger is located between two successive circles with radius $l(k)$ and $l(k+1)$ with respect to a device, then the device must also lie between two circles with radius $l(k)$ and $l(k+1)$ centered at the charger, leading to a constant approximated charging power if the charger covers the device. By this approach, the whole 2D plane is partitioned into a number of subareas. In Figure 6, the charger s_1 falls between the two circles with radius $l(1)$ and $l(2)$ centered at the device o_1, o_2 , and o_3 , and s_1 covers o_1 and o_2 . Suppose $A_o = \frac{\pi}{2}$ and $\Delta A_o = \frac{\pi}{4}$, the whole 2D plane is divided into 132 subareas. The approximated charging power at o_1 and o_2 from the charger is identical and is equal to $P_r(l(2))$.

Next, we have the following theorems.

Theorem 4.2: Let $\tilde{P}_r(j)$ be the approximated charging power of device o_j , we have the approximation error as

$$1 \leq \frac{P_r(j)}{\tilde{P}_r(j)} \leq 1 + \epsilon_1. \quad (5)$$

Theorem 4.3: The number of partitioned subareas is subject to $Z = O(N^2 \epsilon_1^{-2})$.

B. Dominating Coverage Set (DCS) Extraction

After the area discretization, the power from any charger to its surrounding devices is approximated to be constant in each subarea. Consequently, we only need to consider the coverage relationship between chargers and devices in each subarea, which depends on both positions and orientations of chargers. In this subsection, we show that instead of enumerating all possible covered sets of devices in each subarea, we only need to consider a limited number of representative covered sets of devices, which are formally defined as Dominating Coverage Sets (DCSs), and determine their corresponding strategies. We

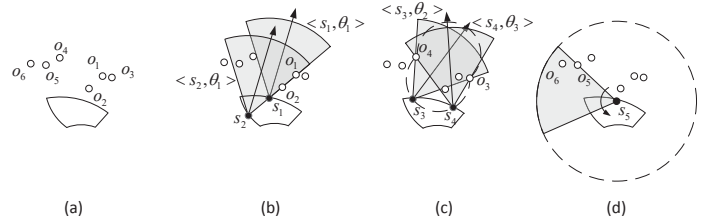


Fig. 7: A toy example of DCS extraction for area case

name the procedure of finding DCSs as *DCS extraction*. Our ultimate goal is to reduce the problem to a combinatorial optimization problem of finding M strategies among a limited number of strategies obtained by DCS extraction.

1) *Preliminaries*: To begin with, we give the following definitions.

Definition 4.2: Given two strategies $\langle s_1, \theta_1 \rangle, \langle s_2, \theta_2 \rangle$ and their covered device sets O_1 and O_2 . If $O_2 = O_1$, we say $\langle s_1, \theta_1 \rangle$ is equivalent to $\langle s_2, \theta_2 \rangle$, or $\langle s_1, \theta_1 \rangle \equiv \langle s_2, \theta_2 \rangle$; if $O_2 \subset O_1$, we say $\langle s_1, \theta_1 \rangle$ dominates $\langle s_2, \theta_2 \rangle$, or $\langle s_1, \theta_1 \rangle \succ \langle s_2, \theta_2 \rangle$; and if $O_2 \subseteq O_1$, we define $\langle s_1, \theta_1 \rangle \succeq \langle s_2, \theta_2 \rangle$.

Definition 4.3: Given a set of devices O_i covered by a strategy $\langle s_i, \theta_i \rangle$, if there doesn't exist a strategy $\langle s_j, \theta_j \rangle$ such that $\langle s_j, \theta_j \rangle \succ \langle s_i, \theta_i \rangle$, then O_i is a *Dominating Coverage Set* (DCS).

In addition, for a given subarea, it is possible that only a few devices can be charged by a charger inside a given subarea, which we formally define as follows.

Definition 4.4: The *candidate covered set of devices* \hat{O}_i of the subarea F_i are those devices that can be charged with non-zero charging power by a charger in F_i .

Apparently, any DCS for a subarea is a subset of the candidate covered set of devices \hat{O}_i .

As choosing DCSs is always better than choosing its subsets, we focus on finding all possible DCSs as well as their corresponding strategies. In what follows, we first consider a special case in which the subarea becomes a point as multiple concentric circles intersect at this point, to facilitate the following analysis. We then study the general case.

2) *DCS Extraction for Point Case*: We only sketch the algorithm for DCS extraction for point case to save space. The algorithm rotates a device on the point such that its orientation varies from 0 to 2π . During the process, it tracks the current set of covered devices, and identifies and records all the DCSs.

3) *DCS Extraction for Area Case*: Next, we consider how to extract DCSs given a general subarea F_i . We present the details of the algorithm in Algorithm 1. Figure 7 shows an example of how the algorithm operates. Given six devices and the subarea as shown in Figure 7(a), we first draw lines passing through each pair of devices, such as o_1 and o_2 in Figure 7(b), and cross the boundaries of the subarea at points s_1 and s_2 , then we obtain two DCSs $\{o_1, o_2\}$ and $\{o_1, o_2, o_4, o_5\}$ as well as their strategies $\langle s_1, \theta_1 \rangle$ and $\langle s_2, \theta_1 \rangle$, respectively. Next, we also draw arcs passing each pair of devices like o_3 and o_4 as shown in Figure 7(c), and find two DCSs $\{o_1, o_3, o_4\}$ and $\{o_1, o_2, o_3, o_4\}$ and their strategies

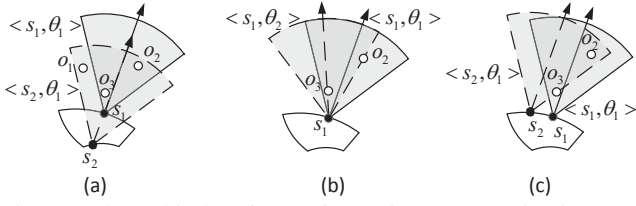


Fig. 8: Three kinds of transformation: (a) Projection, (b) Rotation, (c) Translation

Algorithm 1: DCS Extraction for Area Case

Input: The subarea F_i , the candidate covered set of devices \hat{O}_i

Output: All DCSs

- 1 **for** all pairs of devices, say o_1 and o_2 , in \hat{O}_i **do**
 - 2 Draw a straight line passing through o_1 and o_2 and extend the line to intersect with the subarea's boundaries. Place chargers at these intersection points and adjust their orientations such that o_1 and o_2 lie rightly on its coverage area's clockwise boundary. Then compute the DCSs under the current setting and insert them into the candidate DCS set.
 - 3 Draw two arcs passing through o_1 and o_2 and forming an angle of A_s with respect to them, and then calculate the intersection points of the trajectory and the subarea's boundaries. Place chargers at these intersection points and adjust their orientations such that o_1 and o_2 lie rightly on its coverage area's two boundaries, respectively. Then compute the DCSs under this setting and insert them into the candidate DCS set.
 - 4 Randomly select a point s_j at the boundary of the subarea, perform the algorithm for DCS extraction for point case and add the results to the candidate DCS set.
 - 5 Identify and remove all the DCSs which are subsets of some DCSs in the candidate DCS set.
-

$\langle s_3, \theta_2 \rangle$ and $\langle s_4, \theta_3 \rangle$, respectively. Finally, we randomly choose a point s_5 on the boundaries, as Figure 7(d) illustrates, and perform the algorithm of DCS extraction for point case to further find DCSs. At the final step, $\{o_1, o_2\}$ and $\{o_1, o_3, o_4\}$ can be removed as they are subsets to $\{o_1, o_2, o_4, o_5\}$ and $\{o_1, o_2, o_3, o_4\}$, respectively.

Next, we define three transformations of strategies.

Definition 4.5: (Projection) Given a strategy $\langle s_1, \theta_1 \rangle$, move the charger along the reverse direction of its orientation until reaching some point s_2 on the boundary of the subarea while keeping its orientation unchanged, i.e., $\langle s_2, \theta_1 \rangle = f_{\perp}(\langle s_1, \theta_1 \rangle)$.

Definition 4.6: (Rotation) Given a strategy $\langle s_1, \theta_1 \rangle$, rotate the charger from θ_1 to θ_2 and keep the position unchanged.

Definition 4.7: (Translation) Given a strategy $\langle s_1, \theta_1 \rangle$, move the charger from the position s_1 to another position s_2 and keep the orientation unchanged.

Obviously, the projection transformation is a special case of the translation transformation, and the result is unique. Figure 8 demonstrates the instances of these three transformations. We have the following lemma for projection.

Lemma 4.1: If $\langle s_2, \theta_1 \rangle = f_{\perp}(\langle s_1, \theta_1 \rangle)$, then $\langle s_2, \theta_1 \rangle \succeq \langle s_1, \theta_1 \rangle$.

As shown in Figure 8(a), at the new position s_2 after the projection transformation, the charger can not only cover the

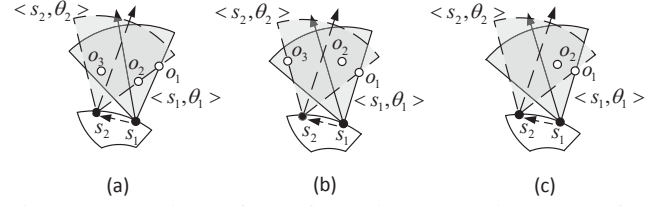


Fig. 9: Three kinds of transformation results in the proof to Theorem 4.4

devices o_2 and o_3 , but also the device o_1 which is not covered before the projection transformation.

According to Lemma 4.1, we can easily get the following crucial corollary.

Corollary 4.1: The DCSs extracted by considering the case wherein chargers located on the boundaries of a subarea are the same as that by considering the whole subarea.

Corollary 4.1 indeed explains why we only need to consider the strategies with positions on the boundaries.

Further, let Γ be the obtained set of DCSs in Algorithm 1, then we have the following theorem.

Theorem 4.4: Given any strategy $\langle s, \theta \rangle$, there exists $\langle s_2, \theta_2 \rangle \in \Gamma$ such that $\langle s_2, \theta_2 \rangle \succeq \langle s, \theta \rangle$.

Proof: To begin with, from Corollary 4.1, we only need to consider the strategies with their positions lying on the boundaries of the subarea. Then, given such a strategy $\langle s, \theta \rangle$, we perform the following transformation.

First, we fix the position s , and rotate the charger anticlockwise, i.e., perform a rotation transformation, such that there is at least one device, say o_1 , touching the right boundary of the charger's coverage area, as similar to that in Figure 8(b). Suppose the obtained strategy is $\langle s_1, \theta_1 \rangle$ ($s_1 = s$). Obviously, we have $\langle s_1, \theta_1 \rangle \succeq \langle s, \theta \rangle$.

Second, we move the charger along the subarea's boundaries and change its orientation accordingly, and during such process of translation and rotation transformations we guarantee that: (1) the newly obtained strategy $\langle s_2, \theta_2 \rangle$ satisfies $\langle s_2, \theta_2 \rangle \succeq \langle s_1, \theta_1 \rangle$; and (2) the clockwise boundary of the charger's coverage area must cross o_1 . In other words, during the adjustment, any device covered currently should not fall out of the coverage area. Apparently, we shall encounter one of the three possible situations as shown in Figure 9.

Case I: At some position s_2 on the boundary of the subarea, there is some device (e.g., o_2 in Figure 9(a)) that touches the clockwise boundary of the coverage area of $\langle s_2, \theta_2 \rangle$.

Case II: At some position s_2 on the boundary of the subarea, there is some device (e.g., o_3 in Figure 9(b)) that touches the anticlockwise boundary of the coverage area of $\langle s_2, \theta_2 \rangle$.

Case III: Neither the situation in (a) nor that in (b) occurs for any position s_2 on the boundary of the subarea (as shown in Figure 9(c)).

In fact, Case I and II are indeed two critical situations that a device covered by $\langle s_1, \theta_1 \rangle$ is about to fall out of the coverage. In contrast, Case III shows that at any position s_2 on subarea's boundary, $\langle s_2, \theta_2 \rangle$ is equivalent to $\langle s_1, \theta_1 \rangle$ (note that during the transformations a device would never fall out of the coverage

from the arc boundary of the sector area, we omit analysis here to save space).

In Algorithm 1, Step 2 and Step 3 correspond to Case I and II, respectively. At Step 4, randomly selecting a position on the subarea's boundaries and performing the DCS extraction algorithm for point case can find all the DCSs resulted from Case III. Thus, the corresponding covered set of devices of strategy $\langle s_2, \theta_2 \rangle$ must be included in Γ before the reduction of trivial DCSs at the final step, and it is either equivalent to or is dominated by some DCS in the final obtained Γ . Since $\langle s_2, \theta_2 \rangle \succeq \langle s_1, \theta_1 \rangle \succeq \langle s, \theta \rangle$, the result follows. ■

C. Problem Reformulation and Solution

In this subsection, we elaborate on how to select a given number of strategies from the obtained ones in the last subsection to maximize the overall charging utility. Specifically, we first reformulate the problem, then prove its submodularity, and thereby propose an effective algorithm to address the problem.

For any DCS in the set of all obtained DCSs from all subareas which is still denoted by Γ , we can compute the power received by each device correspondingly. Let x_i be a binary indicator denoting whether the i_{th} strategy in Γ is selected or not. The problem **P1** can be reformulated as

$$\begin{aligned} \max \quad & \frac{\Delta A_o}{2\pi N} \sum_{j=1}^N \sum_{q=1}^{\frac{2\pi}{\Delta A_o}} \mathcal{U} \left(\sum_{\langle s_i, \theta_i \rangle \in \Gamma} x_i \tilde{P}_r(s_i, \theta_i, o_j, q\Delta A_o) \right) \\ \text{s.t.} \quad & \sum_{i=1}^{|\Gamma|} x_i = M \quad (x_i \in \{0, 1\}). \end{aligned} \quad (6)$$

Now **P2** becomes a combinatorial optimization problem. Before addressing **P2**, we first give the following definitions to assist further analysis.

Definition 4.8: [24] Let S be a finite ground set. A real-valued set function $f : 2^S \rightarrow \mathbb{R}$ is normalized, monotonic and submodular if and only if it satisfies the following conditions, respectively: (1) $f(\emptyset) = 0$; (2) $f(A \cup \{e\}) - f(A) \geq 0$ for any $A \subseteq S$ and $e \in S \setminus A$; (3) $f(A \cup \{e\}) - f(A) \geq f(B \cup \{e\}) - f(B)$ for any $A \subseteq B \subseteq S$ and $e \in S \setminus B$.

Definition 4.9: [24] A Matroid \mathcal{M} is a strategy $\mathcal{M} = (S, L)$ where S is a finite ground set, $L \subseteq 2^S$ is a collection of independent sets, such that: (1) $\emptyset \in L$; (2) if $X \subseteq Y \in L$, then $X \in L$; (3) if $X, Y \in L$, and $|X| < |Y|$, then $\exists y \in Y \setminus X$, $X \cup \{y\} \in L$.

Definition 4.10: [24] Given a finite set S and an integer k . A uniform matroid $\mathcal{M} = (S, L)$ is a matroid where $L = \{X \subseteq S : |X| \leq k\}$.

Based on these definitions, problem **P2** can be rewritten as

$$\begin{aligned} \max \quad & f(X) = \frac{\Delta A_o}{2\pi N} \sum_{j=1}^N \sum_{q=1}^{\frac{2\pi}{\Delta A_o}} \mathcal{U} \left(\sum_{\langle s_i, \theta_i \rangle \in X} \tilde{P}_r(s_i, \theta_i, o_j, q\Delta A_o) \right) \\ \text{s.t.} \quad & X \in L, \\ & L = \{X \subseteq \Gamma : |X| \leq M\}. \end{aligned} \quad (7)$$

Algorithm 2: Strategy Selection

Input: The number of chargers M , DCS set Γ , objective function $f(X)$

Output: Strategy set X

```

1  $X = \emptyset$ .
2 while  $|X| \leq M$  do
3    $e^* = \arg \max_{e \in \Gamma \setminus X} f(X \cup \{e\}) - f(X)$ .
4    $X = X \cup \{e^*\}$ .
```

Lemma 4.2: The objective function $f(X)$ in **P3** is a monotone submodular function, and the constraint is a uniform matroid constraint.

Therefore, our reformulated problem falls into the scope of the problem of maximizing a monotone submodular function subject to matroid constraints, which allows a greedy algorithm to achieve a good approximation [24]. We describe the algorithm of selecting strategies in Algorithm 2. At each step, Algorithm 2 greedily adds a strategy e^* to X such that the increment of the function $f(\cdot)$ is maximized.

D. Theoretical Analysis

Theorem 4.5: Setting $\Delta A_o = \frac{\pi\beta^2 P_{th}}{\alpha N \lceil \frac{\pi}{\Delta A_o} \rceil \lceil \frac{P_{th}}{\alpha/\beta^2} \rceil} \epsilon$ and $\epsilon_1 = \frac{\epsilon}{2}$,

the PLOT algorithm achieves an approximation ratio of $1 - 1/e - \epsilon$, and its time complexity is $O(M\epsilon^{-4}N^4 + M\epsilon^{-3}N^5)$.

Proof: Let Γ_1^* and Γ_2^* denote the set of strategies of all M chargers under the optimal solution to the problem **P1** and the reformulated problem **P2**, respectively, and Γ_2 denote the obtained strategies of PLOT to the problem **P2** (or **P3**). First, by Lemma 4.2 and the fact that the greedy algorithm of maximizing a monotone submodular function subject to a uniform matroid achieves $1 - 1/e$ approximation ratio [24], the approximation ratio of Algorithm 2 is thus $1 - 1/e$, namely,

$$\begin{aligned} & \frac{\Delta A_o}{2\pi N} \sum_{j=1}^N \sum_{q=1}^{\frac{2\pi}{\Delta A_o}} \mathcal{U} \left(\sum_{\langle s_i, \theta_i \rangle \in \Gamma_2} \tilde{P}_r(s_i, \theta_i, o_j, q\Delta A_o) \right) \\ & \geq (1 - \frac{1}{e}) \frac{\Delta A_o}{2\pi N} \sum_{j=1}^N \sum_{q=1}^{\frac{2\pi}{\Delta A_o}} \mathcal{U} \left(\sum_{\langle s_i, \theta_i \rangle \in \Gamma_2^*} \tilde{P}_r(s_i, \theta_i, o_j, q\Delta A_o) \right). \end{aligned} \quad (8)$$

Further, by Eq. (5), we have $\tilde{P}_r^{OPT}(i) \geq \frac{1}{1+\epsilon_1} P_r^{OPT}(i)$.

Second, assume Γ_4^* is the optimal solution to the following problem

$$\begin{aligned} \text{(P4)} \quad \max \quad & \frac{\Delta A_o}{2\pi N} \sum_{j=1}^N \sum_{q=1}^{\frac{2\pi}{\Delta A_o}} \mathcal{U} \left(\sum_{i=1}^M P_r(s_i, \theta_i, o_j, q\Delta A_o) \right) \\ \text{s.t.} \quad & s_i \in \Omega, 0 \leq \theta_i < 2\pi. \end{aligned} \quad (9)$$

According to Theorem 4.1, we have $\tilde{P}_r(s_i, \theta_i, o_j, q\Delta A_o) \geq \frac{1}{1+\epsilon_1} P_r(s_i, \theta_i, o_j, q\Delta A_o)$. Then, by the property of the charging utility function, we have

$$\begin{aligned} & \frac{\Delta A_o}{2\pi N} \sum_{j=1}^N \sum_{q=1}^{\frac{2\pi}{\Delta A_o}} \mathcal{U} \left(\sum_{\langle s_i, \theta_i \rangle \in \Gamma_2^*} \tilde{P}_r(s_i, \theta_i, o_j, q\Delta A_o) \right) \\ & \geq \frac{\Delta A_o}{2\pi N} \sum_{j=1}^N \sum_{q=1}^{\frac{2\pi}{\Delta A_o}} \mathcal{U} \left(\sum_{\langle s_i, \theta_i \rangle \in \Gamma_4^*} \tilde{P}_r(s_i, \theta_i, o_j, q\Delta A_o) \right) \\ & \geq \frac{\Delta A_o}{2\pi N} \sum_{j=1}^N \sum_{q=1}^{\frac{2\pi}{\Delta A_o}} \mathcal{U} \left(\sum_{\langle s_i, \theta_i \rangle \in \Gamma_4^*} \frac{1}{1+\epsilon_1} P_r(s_i, \theta_i, o_j, q\Delta A_o) \right) \\ & \geq \frac{1}{1+\epsilon_1} \frac{\Delta A_o}{2\pi N} \sum_{j=1}^N \sum_{q=1}^{\frac{2\pi}{\Delta A_o}} \mathcal{U} \left(\sum_{\langle s_i, \theta_i \rangle \in \Gamma_4^*} P_r(s_i, \theta_i, o_j, q\Delta A_o) \right). \end{aligned} \quad (10)$$

Note that the first inequality is because Γ_2^* is optimal under the setting of **P2**.

Third, suppose Γ_5^* is the optimal solution to the new problem **P5** which is same as **P1** except that the receiving angle of rechargeable devices is slightly reduced to $A_o - \Delta A_o$. Accordingly, we use $P'_r(s_i, \theta_i, o_j, \phi_j)$ to denote the charging power from charger s_i with orientation θ_i to device o_j with orientation ϕ_j under the settings of **P5**. Then we have:

$$\begin{aligned}
 & \frac{\Delta A_o}{2\pi N} \sum_{j=1}^N \sum_{q=1}^{\frac{2\pi}{\Delta A_o}} \mathcal{U}(\sum_{\langle s_i, \theta_i \rangle \in \Gamma_4^*} P_r(s_i, \theta_i, o_j, q\Delta A_o)) \\
 & \geq \frac{\Delta A_o}{2\pi N} \sum_{j=1}^N \sum_{q=1}^{\frac{2\pi}{\Delta A_o}} \mathcal{U}(\sum_{\langle s_i, \theta_i \rangle \in \Gamma_5^*} P_r(s_i, \theta_i, o_j, q\Delta A_o)) \\
 & = \frac{1}{N} \sum_{j=1}^N (\frac{1}{2\pi} \sum_{q=1}^{\frac{2\pi}{\Delta A_o}} \mathcal{U}(\sum_{\langle s_i, \theta_i \rangle \in \Gamma_5^*} P_r(s_i, \theta_i, o_j, q\Delta A_o)) \Delta A_o) \\
 & \geq \frac{1}{N} \sum_{j=1}^N (\frac{1}{2\pi} \sum_{q=1}^{\frac{2\pi}{\Delta A_o}} \int_{(q-\frac{1}{2})\Delta A_o}^{(q+\frac{1}{2})\Delta A_o} \mathcal{U}(\sum_{\langle s_i, \theta_i \rangle \in \Gamma_5^*} P'_r(s_i, \theta_i, o_j, \phi)) d\phi) \\
 & = \frac{1}{2\pi N} \sum_{j=1}^N \int_0^{2\pi} \mathcal{U}(\sum_{\langle s_i, \theta_i \rangle \in \Gamma_5^*} P'_r(s_i, \theta_i, o_j, \phi)) d\phi. \tag{11}
 \end{aligned}$$

Note that the last inequality is because the receiving area with receiving angle $A_o - \Delta A_o$ and orientation $\phi \in [(q - \frac{1}{2})\Delta A_o, (q + \frac{1}{2})\Delta A_o]$ is always covered by the receiving area with receiving angle A_o and orientation $q\Delta A_o$.

Fourth, we evaluate the performance gap between the optimal solutions to **P1** and **P5**.

$$\begin{aligned}
 & \frac{1}{2\pi N} \sum_{j=1}^N \int_0^{2\pi} \mathcal{U}(\sum_{\langle s_i, \theta_i \rangle \in \Gamma_1^*} P_r(s_i, \theta_i, o_j, \phi)) d\phi \\
 & - \frac{1}{2\pi N} \sum_{j=1}^N \int_0^{2\pi} \mathcal{U}(\sum_{\langle s_i, \theta_i \rangle \in \Gamma_5^*} P'_r(s_i, \theta_i, o_j, \phi)) d\phi \\
 & \leq \frac{1}{2\pi N} \sum_{j=1}^N \int_0^{2\pi} [\mathcal{U}(\sum_{\langle s_i, \theta_i \rangle \in \Gamma_1^*} P_r(s_i, \theta_i, o_j, \phi)) \\
 & - \mathcal{U}(\sum_{\langle s_i, \theta_i \rangle \in \Gamma_5^*} P'_r(s_i, \theta_i, o_j, \phi))] d\phi \\
 & \leq \frac{1}{2\pi N} \sum_{j=1}^N \int_0^{2\pi} c_u (\sum_{\langle s_i, \theta_i \rangle \in \Gamma_1^*} P_r(s_i, \theta_i, o_j, \phi) \\
 & - \sum_{\langle s_i, \theta_i \rangle \in \Gamma_5^*} P'_r(s_i, \theta_i, o_j, \phi)) d\phi \\
 & = \frac{c_u}{2\pi N} \sum_{j=1}^N \sum_{\substack{\langle s_i, \theta_i \rangle \in \Gamma_1^* \\ \|s_i o_j\| \leq D}} \frac{\alpha}{(\|s_i o_j\| + \beta)^2} \cdot A_o \\
 & - \frac{c_u}{2\pi N} \sum_{j=1}^N \sum_{\substack{\langle s_i, \theta_i \rangle \in \Gamma_5^* \\ \|s_i o_j\| \leq D}} \frac{\alpha}{(\|s_i o_j\| + \beta)^2} \cdot (A_o - \Delta A_o) \\
 & \leq \frac{c_u \alpha M}{2\pi \beta^2} \Delta A_o. \tag{12}
 \end{aligned}$$

Next, to bound the performance of the best solution to **P1**, we consider the following baseline placement scheme first. This scheme deploys chargers to cover given points in sequence. For each point, it uniformly divides its 2π span angle into $\lceil \frac{2\pi}{A_o} \rceil$ sectors. For each sector, it puts chargers one by one in the sector very close to the point until the aggregated power at the point exceeds P_{th} , which needs at most $\lceil \frac{P_{th}}{\alpha/\beta^2} \rceil$ chargers; and then moves to the next sector. After all the sectors for a

point are covered, the scheme turns to cover another point. Obviously, even in the extreme case where each charger can cover only one single point, the scheme still achieves a utility of $M \cdot \frac{1}{N} \cdot \frac{c_u P_{th}}{\lceil \frac{2\pi}{A_o} \rceil \lceil \frac{P_{th}}{\alpha/\beta^2} \rceil}$. Then, we have

$$\begin{aligned}
 & \frac{1}{2\pi N} \sum_{j=1}^N \int_0^{2\pi} \mathcal{U}(\sum_{\langle s_i, \theta_i \rangle \in \Gamma_1^*} P_r(s_i, \theta_i, o_j, \phi)) d\phi \\
 & - \frac{1}{2\pi N} \sum_{j=1}^N \int_0^{2\pi} \mathcal{U}(\sum_{\langle s_i, \theta_i \rangle \in \Gamma_5^*} P'_r(s_i, \theta_i, o_j, \phi)) d\phi \\
 & \leq \frac{\alpha N \lceil \frac{2\pi}{A_o} \rceil \lceil \frac{P_{th}}{\alpha/\beta^2} \rceil}{2\pi \beta^2 P_{th}} \Delta A_o \cdot \frac{c_u P_{th} M}{N \lceil \frac{2\pi}{A_o} \rceil \lceil \frac{P_{th}}{\alpha/\beta^2} \rceil} \\
 & \leq \frac{\alpha N \lceil \frac{2\pi}{A_o} \rceil \lceil \frac{P_{th}}{\alpha/\beta^2} \rceil}{2\pi \beta^2 P_{th}} \Delta A_o \\
 & \cdot \frac{1}{2\pi N} \sum_{j=1}^N \int_0^{2\pi} \mathcal{U}(\sum_{\langle s_i, \theta_i \rangle \in \Gamma_1^*} P_r(s_i, \theta_i, o_j, \phi)) d\phi, \tag{13}
 \end{aligned}$$

and thereby

$$\begin{aligned}
 & \frac{1}{2\pi N} \sum_{j=1}^N \int_0^{2\pi} \mathcal{U}(\sum_{\langle s_i, \theta_i \rangle \in \Gamma_5^*} P'_r(s_i, \theta_i, o_j, \phi)) d\phi \\
 & \geq (1 - \frac{\alpha N \lceil \frac{2\pi}{A_o} \rceil \lceil \frac{P_{th}}{\alpha/\beta^2} \rceil}{2\pi \beta^2 P_{th}} \Delta A_o) \\
 & \cdot \frac{1}{2\pi N} \sum_{j=1}^N \int_0^{2\pi} \mathcal{U}(\sum_{\langle s_i, \theta_i \rangle \in \Gamma_1^*} P_r(s_i, \theta_i, o_j, \phi)) d\phi. \tag{14}
 \end{aligned}$$

Combining Inequality (8), (10), (11), and (14), we obtain

$$\begin{aligned}
 & \frac{\Delta A_o}{2\pi N} \sum_{j=1}^N \sum_{q=1}^{\frac{2\pi}{\Delta A_o}} \mathcal{U}(\sum_{\langle s_i, \theta_i \rangle \in \Gamma_2} \tilde{P}_r(s_i, \theta_i, o_j, q\Delta A_o)) \\
 & \geq (1 - 1/e) \cdot \frac{1}{1 + \epsilon_1} \cdot (1 - \frac{\alpha N \lceil \frac{2\pi}{A_o} \rceil \lceil \frac{P_{th}}{\alpha/\beta^2} \rceil}{2\pi \beta^2 P_{th}} \Delta A_o) \\
 & \cdot \frac{1}{2\pi N} \sum_{j=1}^N \int_0^{2\pi} \mathcal{U}(\sum_{\langle s_i, \theta_i \rangle \in \Gamma_1^*} P_r(s_i, \theta_i, o_j, \phi)) d\phi \\
 & \geq (1 - 1/e - \epsilon_1 - \frac{\alpha N \lceil \frac{2\pi}{A_o} \rceil \lceil \frac{P_{th}}{\alpha/\beta^2} \rceil}{2\pi \beta^2 P_{th}} \Delta A_o) \\
 & \cdot \frac{1}{2\pi N} \sum_{j=1}^N \int_0^{2\pi} \mathcal{U}(\sum_{\langle s_i, \theta_i \rangle \in \Gamma_1^*} P_r(s_i, \theta_i, o_j, \phi)) d\phi. \tag{15}
 \end{aligned}$$

Hence, if we set $\epsilon_1 = \frac{\epsilon}{2}$ and $\Delta A_o = \frac{\pi \beta^2 P_{th}}{\alpha N \lceil \frac{2\pi}{A_o} \rceil \lceil \frac{P_{th}}{\alpha/\beta^2} \rceil} \epsilon$, then the approximation ratio of the PLOT algorithm is $1 - 1/e - \epsilon$.

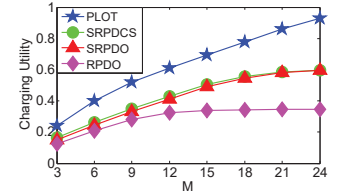
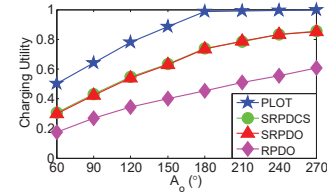
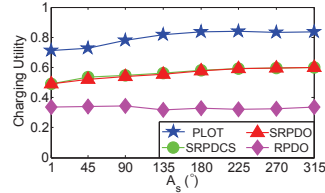
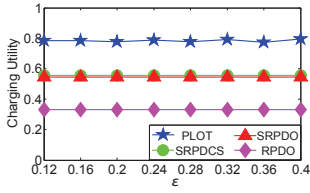
We omit the time complexity analysis to save space. ■

V. SIMULATION RESULTS

In this section, we conduct simulations to verify the performance of the PLOT algorithm by comparing it with three other randomized algorithms in terms of error threshold ϵ , charging angle A_s , receiving angle A_o and number of chargers M .

A. Evaluation Setup

In our simulation, the target field is a $40m \times 40m$ square area, and the points are uniformly distributed in this area. If no otherwise stated, we set $\alpha = 100$, $\beta = 40$, $D = 6m$, $N = 12$, $P_{th} = 0.05W$, $\epsilon = 0.2$, $A_s = \pi/2$, $A_o = 2\pi/3$, and $M = 18$, respectively. Moreover, each charging utility result is obtained by averaging results for 100 random topologies.


 Fig. 10: ϵ vs. charging utility Fig. 11: A_s vs. charging utility

B. Baseline Setup

As there are no approaches available to wireless charger placement for directional charging utility optimization, we develop three algorithms named Randomized Position and Discretized Orientation (RPDO), Selected Randomized Position and Discretized Orientation (SRPDO), and Selected Randomized Position with Dominating Coverage Sets (SRPDCS) for comparison. RPDO randomly distributes directional chargers in the target field, and picks the direction of each charger among eight candidate angles, *i.e.*, $0, \pi/4, \dots, 7\pi/4$ if $A_s \geq \pi/4$, and among $0, A_s, \dots, \lfloor \frac{2\pi}{A_s} \rfloor A_s$ if $A_s < \pi/4$. SRPDO improves RPDO by selecting positions with at least one device within the distance of D when generating random positions. SRPDCS improves SRPDO by applying the algorithm for DCS extraction for point case to generate candidate orientations. All these algorithms use a greedy method to sequentially choose M strategies.

C. Performance Comparison

1) *Impact of Error Threshold ϵ* : Our simulation results show that on average, PLOT outperforms SRPDCS, SRPDO, and RPDO by 41.4%, 43.8%, and 138.0%, respectively, in terms of ϵ . Figure 10 shows that the charging utility of PLOT fluctuates slightly as ϵ grows, but is always larger than 0.77. Thus, we can reasonably choose a large ϵ to reduce the running time of PLOT without noticeably degrading its performance.

2) *Impact of Charging Angle A_s* : Our simulation results show that on average PLOT outperforms SRPDCS, SRPDO, and RPDO by 41.7%, 42.9%, and 140.95%, respectively, in terms of A_s . Figure 11 shows the charging utility of PLOT, SRPDCS, or SRPDO increases slowly with A_s , while that of RPDO keeps relatively stable at a low level. This is because the density of devices in our simulation is relatively low and most chargers can only cover one single device regardless of their chosen orientation for utility optimization, therefore, the charging angle A_s has little impact on the charging utility.

3) *Impact of Receiving Angle A_o* : Our simulation results show that on average, PLOT outperforms SRPDCS, SRPDO, and RPDO by 36.4%, 37.9%, and 115.8%, respectively, in terms of A_o . Figure 12 shows that the charging utility of three algorithms increases monotonically with A_o . The charging utility of our algorithm first increases at a faster speed than the other three algorithms and approaches 1 when A_o increases from 60° to 180° , and then keeps stable.

4) *Impact of Number of Chargers M* : Our simulation results show that on average, PLOT outperforms SRPDCS, SRPDO, and RPDO by 46.3%, 51.9%, and 113.1%, respectively, in terms of M . Figure 13 shows that the charging utility of PLOT invariably increases with M until it approaches 1, while

that of RPDO, SRPDCS, and SRPDO increase to about 0.35, 0.6, and 0.6, respectively, and then keeps relatively stable.

D. Insights

In this subsection, we study the impact of uniformness of position distribution for devices on the overall charging utility. Suppose there are 12 devices distributed in a $40m \times 40m$ square area and $A_o = 2\pi/3$ and $A_s = \pi/2$. The position of the devices follows a 2D Gaussian distribution with both x - and y - coordinates being randomly selected from a Gaussian distribution with $\mu = 20$. We vary the standard deviation σ_x for x -coordinate and σ_y for y -coordinate both from 3 to 12, and depict the results in Figure 14. Note that each point on the surface denotes an average value of 100 experimental results. We observe that generally the charging utility decreases monotonically when either σ_x or σ_y increases. Indeed, when σ_x or σ_y increases, the position distribution of devices appears more random, and approaches to uniform distribution. Thus we claim that the uniformness of position distribution for devices negatively impacts the charging utility.

VI. FIELD EXPERIMENTS

In this section, we conduct field experiments to evaluate the performance of the PLOT algorithm.

A. Testbed

As shown in Figure 15, our testbed consists of five TX91501 power transmitters produced by Powercast [18], ten rechargeable sensor nodes, and an AP connecting to a laptop to report the collected data from sensor nodes. The rechargeable sensor nodes are placed in the region of a $240cm \times 240cm$ square area whose coordinates are (140, 135), (167, 140), (233, 185), (140, 205), (133, 215), (127, 235), (147, 230), (167, 220), (170, 238), and (180, 213), respectively. We require that all the chargers should be placed in the area bounded by two dotted squares with side lengths 360 cm and 240 cm as shown in Figure 15. We can achieve this requirement by filtering the obtained results of Algorithm 1 and keeping those strategies with positions lie in the confined area. Note that we set $P_{th} = 5mW$, and ϵ such that $\Delta A_o = 20^\circ$.

B. Experimental Results

The placed chargers for PLOT, SRPDO, and SRPDCS are shown in the blue, red, and green sectors, respectively, in Figure 15. We can observe that PLOT places chargers in the four corners of the area, while SRPDO and SRPDCS place chargers more arbitrarily with many chargers placed close to each other with similar orientations. Figure 16 shows the charging utility for each device for the three algorithms. We can see that PLOT always has higher utility than other two algorithms for each device. Our algorithm PLOT outperforms SRPDO and SRPDCS by at least 23.0% and 27.6%, and by

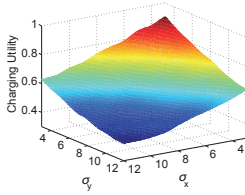


Fig. 14: Insights

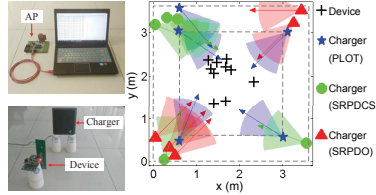


Fig. 15: Testbed

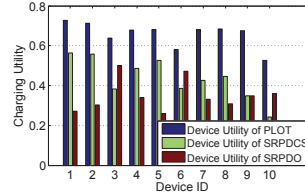


Fig. 16: Utility of devices

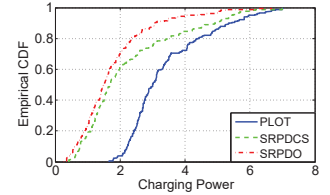


Fig. 17: Empirical CDF

98.3% and 56.6% on average, respectively. Moreover, Figure 17 shows the CDFs of received charging powers for devices at 10 positions with $360^\circ/\Delta A_o = 18$ possible orientations for the three algorithms. We can see that devices for PLOT achieve much larger charging power compared to others. For example, the percentage of devices with charging power less than $2mW$ occupies only 3.9% for PLOT, while the percentages for SRPDO and SRPDCS are up to 70.0% and 61.1%, respectively.

VII. DISCUSSION

Deploying minimum wireless chargers to achieve a required charging utility. The solution is nearly the same as the PLOT algorithm, except that in Algorithm 2, we greedily select strategies for chargers one by one until a required charging utility is achieved, and then output the selected strategies. According to the classical results in [25], the adapted algorithm based on Algorithm 2 achieves $\frac{1}{\ln n}$ approximation ratio, where n is the number of candidate strategies. By similar analysis, we can prove that the overall solution can still achieve $\frac{1}{\ln n}$ approximation ratio. Despite that n is typically a large value, we can try to reduce n by removing unnecessary strategies to improve the performance guarantee.

Determined topology of rechargeable devices. When the topology of devices is determined with known positions and orientations, we can substitute the devices for the set of devices we used to approximate the expected charging utility for a point. Then, we perform the PLOT algorithm in the same way, and can still obtain a $1 - 1/e - \epsilon$ approximation algorithm.

VIII. CONCLUSION

The key novelty of this paper is on proposing the first scheme for wireless charger placement with optimized charging utility. The key contribution of this paper is building the empirical directional charging model, developing an approximation algorithm, and conducting field experiments for evaluation. The key technical depth of this paper is in making the original nonlinear and continuous optimization problem almost linear and discrete by presenting the techniques of area discretization and Dominating Coverage Set extraction, and proving that the reformulated problem is a problem of maximizing a monotone submodular function subject to matroid constraints. Our simulation and experimental results show that our proposed scheme achieves good performance and can outperform the other algorithms by at least 46.3%.

ACKNOWLEDGMENT

This work is partially supported by the National Natural Science Foundation of China under Grant Numbers 61502229, 61472184, 61321491, 61472252, 61321491, 61672353, and

61373130, and the National Science Foundation under Grant Numbers CNS-1318563, CNS-1524698, and CNS-1421407, an IIP-1632051, and the Jiangsu High-level Innovation and Entrepreneurship (Shuangchuang) Program, and China 973 projects (2014CB340303). Alex X. Liu is also affiliated with the Department of Computer Science and Engineering, Michigan State University, East Lansing, MI, USA.

REFERENCES

- [1] "https://www.wirelesspowerconsortium.com/."
- [2] "https://www.electronics.ca/store/wireless-power-transmission-market-forecast-analysis.html."
- [3] R. Zhang *et al.*, "MIMO broadcasting for simultaneous wireless information and power transfer," *IEEE Transactions on Wireless Communications*, vol. 12, no. 5, pp. 1989–2001, 2013.
- [4] Z. Ding *et al.*, "Application of smart antenna technologies in simultaneous wireless information and power transfer," *IEEE Communications Magazine*, vol. 53, no. 4, pp. 86–93, 2015.
- [5] "http://www.powercastco.com/pdf/p2110-evb-reva.pdf."
- [6] T. Bai *et al.*, "Coverage and rate analysis for millimeter-wave cellular networks," *IEEE Transactions on Wireless Communications*, vol. 14, no. 2, pp. 1100–1114, 2015.
- [7] L. Wang *et al.*, "Millimeter wave power transfer and information transmission," *IEEE Globecom*, pp. 1–6, 2015.
- [8] S. Bi *et al.*, "Wireless powered communication networks: an overview," *IEEE Wireless Communications*, vol. 23, no. 2, pp. 10–18, 2016.
- [9] S. He *et al.*, "Energy provisioning in wireless rechargeable sensor networks," in *IEEE INFOCOM*, 2011, pp. 2006–2014.
- [10] T.-C. Chiu *et al.*, "Mobility-aware charger deployment for wireless rechargeable sensor networks," in *IEEE APNOMS*, 2012, pp. 1–7.
- [11] H. Dai *et al.*, "Radiation constrained wireless charger placement," in *IEEE INFOCOM*, 2016.
- [12] E. Horster *et al.*, "Approximating optimal visual sensor placement," in *IEEE International Conference on Multimedia and Expo*, 2006, pp. 1257–1260.
- [13] E. Hörster and R. Lienhart, "On the optimal placement of multiple visual sensors," in *ACM VSSN*, 2006, pp. 111–120.
- [14] J. Zhao *et al.*, "Multi-camera surveillance with visual tagging and generic camera placement," in *ACM/IEEE ICDSC*, 2007, pp. 259–266.
- [15] G. Fusco and H. Gupta, "Selection and orientation of directional sensors for coverage maximization," in *IEEE SECON*, 2009, pp. 1–9.
- [16] Y. E. Osais *et al.*, "Directional sensor placement with optimal sensing range, field of view and orientation," *Mobile Networks and Applications*, vol. 15, no. 2, pp. 216–225, 2010.
- [17] X. Han *et al.*, "Deploying directional sensor networks with guaranteed connectivity and coverage," in *IEEE SECON*, 2008, pp. 153–160.
- [18] "www.powercastco.com."
- [19] "http://www.powercastco.com/pdf/tx91501-manual.pdf."
- [20] S. He *et al.*, "Energy provisioning in wireless rechargeable sensor networks," *IEEE Transactions on Mobile Computing*, vol. 12, no. 10, pp. 1931–1942, 2013.
- [21] H. Dai *et al.*, "Safe charging for wireless power transfer," in *IEEE INFOCOM*, 2014, pp. 1105–1113.
- [22] —, "Effective algorithm for placement of directional wireless chargers," *Journal of Software*, vol. 26, no. 7, 2015.
- [23] R. G. Michael and S. J. David, "Computers and intractability: a guide to the theory of np-completeness," *WH Free. Co., San Fr*, 1979.
- [24] S. Fujishige, *Submodular functions and optimization*. Elsevier, 2005, vol. 58.
- [25] V. Chvatal, "A greedy heuristic for the set-covering problem," *Mathematics of operations research*, vol. 4, no. 3, pp. 233–235, 1979.